Real-Time Multiplex Kinase Phosphorylation Sensors in Living Cells

Nur P. Damayanti[1,2,5], Kevin Buno[3], Yi Cui[1,2,6], Sherry L. Voytik-Harbin[2-4], Roberto Pili[5], Jennifer Freeman[7] Joseph M. K. Irudayaraj[1,2*]

[1]Agricultural and Biological Engineering, Purdue University, West Lafayette, Indiana, 47907, USA
[2]Bindley Bioscience Center, Purdue Center for Cancer Research, Purdue University, West Lafayette, Indiana, 47907, USA
[3]Weldon School of Biomedical Engineering, Purdue University, West Lafayette, Indiana, 47907, USA
[4]Department of Basic Medical Sciences, Purdue University, West Lafayette, Indiana, 47907, USA
[5]Indiana University School of Medicine, Indianapolis, Indiana, 46202, USA
[6]Present Address: Earth and Biological Sciences Directorate, Pacific Northwest National Laboratory, Richland, Washington, 99354, USA.
[7]School of Health Sciences, West Lafayette, IN, 47907, USA.

Corresponding author: Joseph M.K. Irudayaraj, email: josephi@purdue.edu

Supporting information.

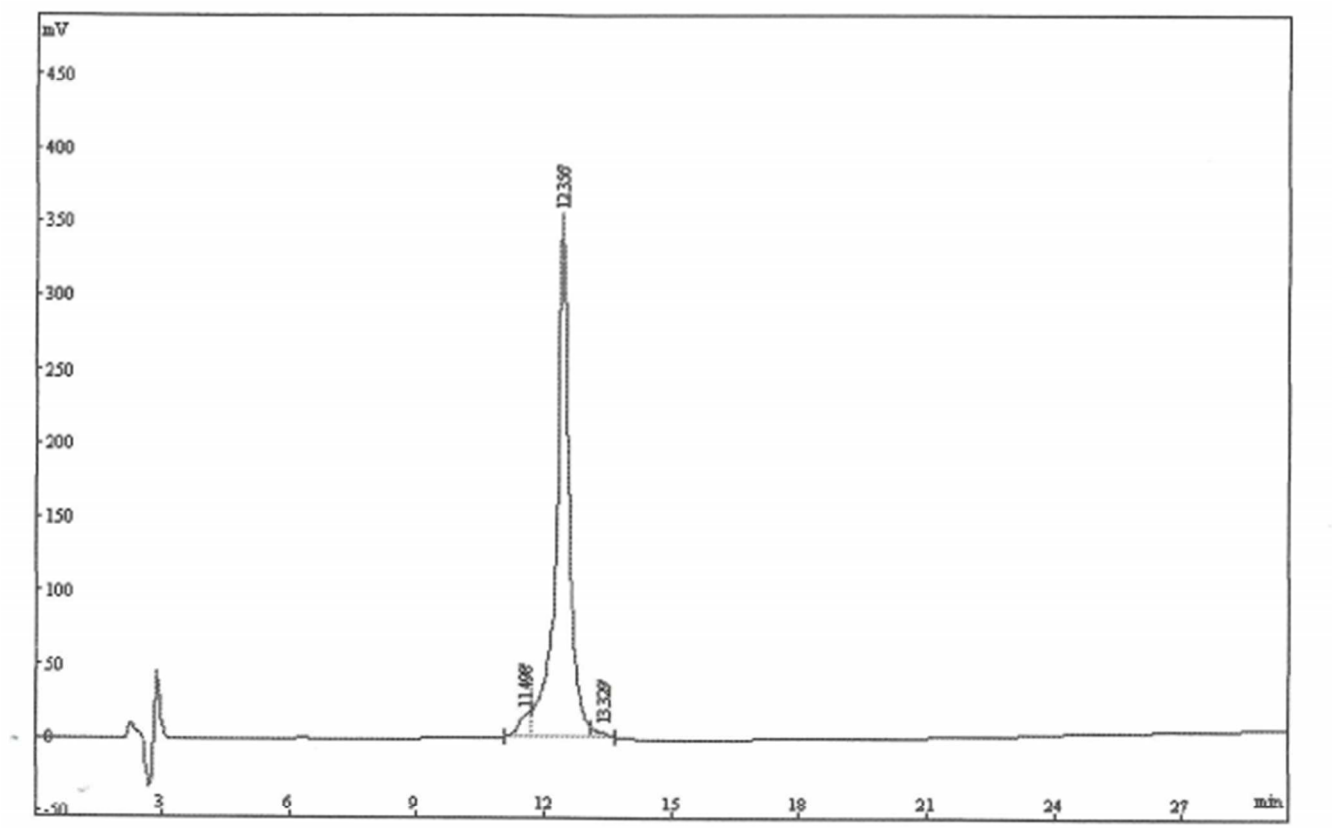

No.	RT	Area%	Area
1	11.498	3.896	310016
2	12.356	95.04	7563128
3	13.329	1.07	85175
Total		100	7958319

Supplementary Figure 1a. HPLC characterization of purified ASOR, ARKRERAYSFK(5FAM)HHARKKRRQRRRPQ.

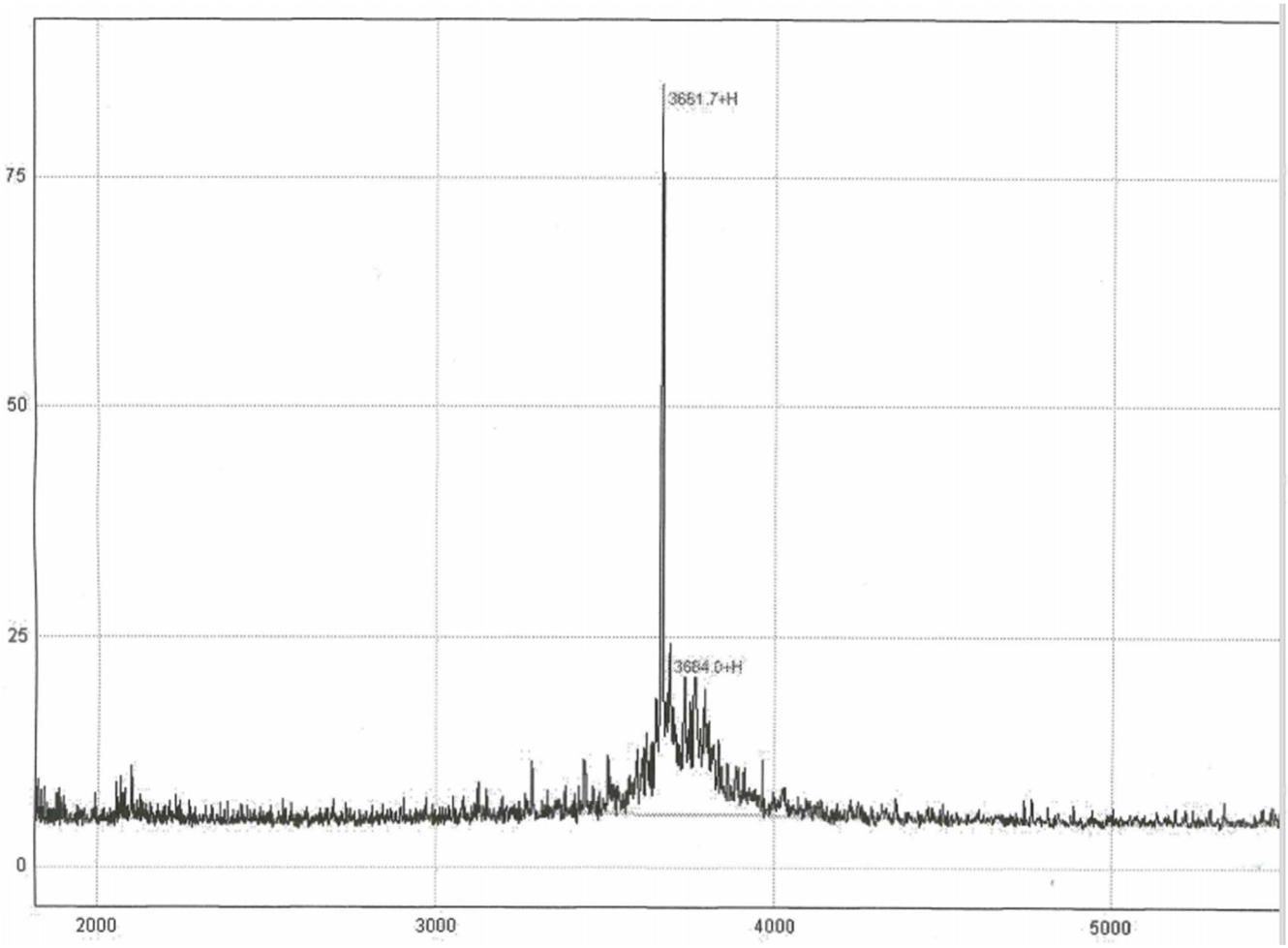

Supplementary Figure 1b. MALDI-TOF characterization of purified ASOR, ARKRERAYSFK(5FAM)HHARKKRRQRRRPQ.

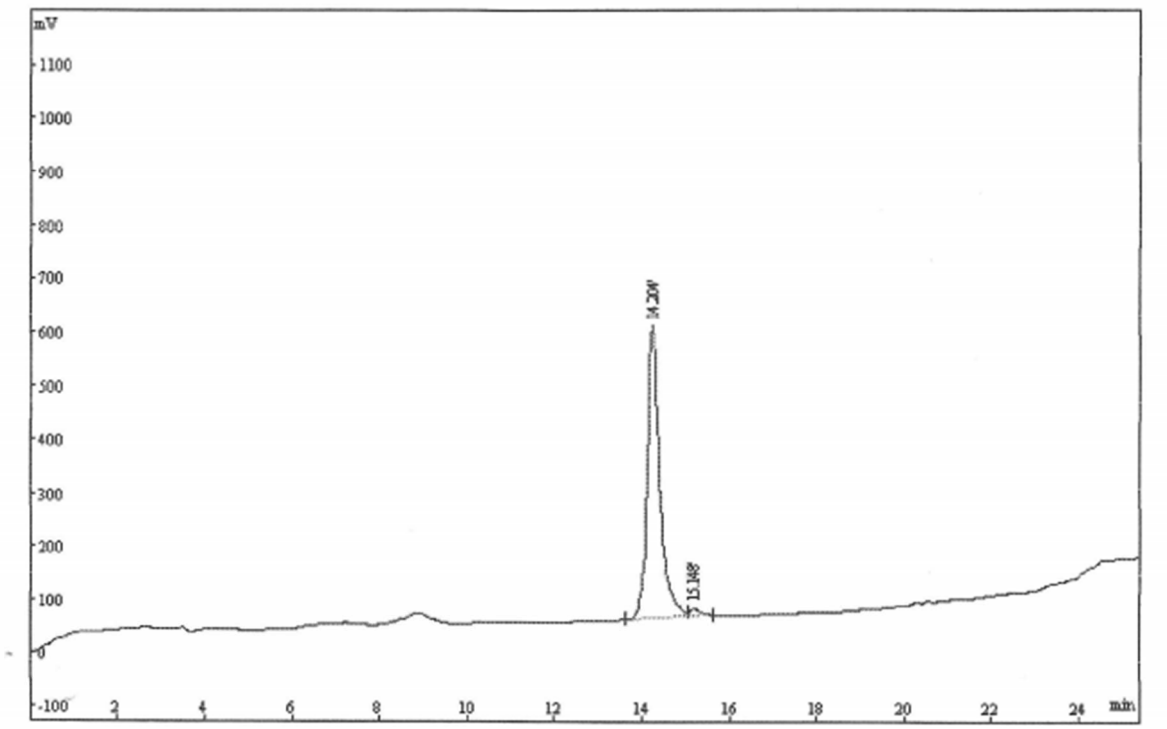

No.	RT	Area%	Area
1	14.204	97.86	11188256
2	15.148	2.139	244553
Total		100	11432809

Supplementary Figure 1c. HPLC characterization of purified VSOR, GRRRAAPEDLYK(5FAM)DFLTGRKKRRQRRRPQ.

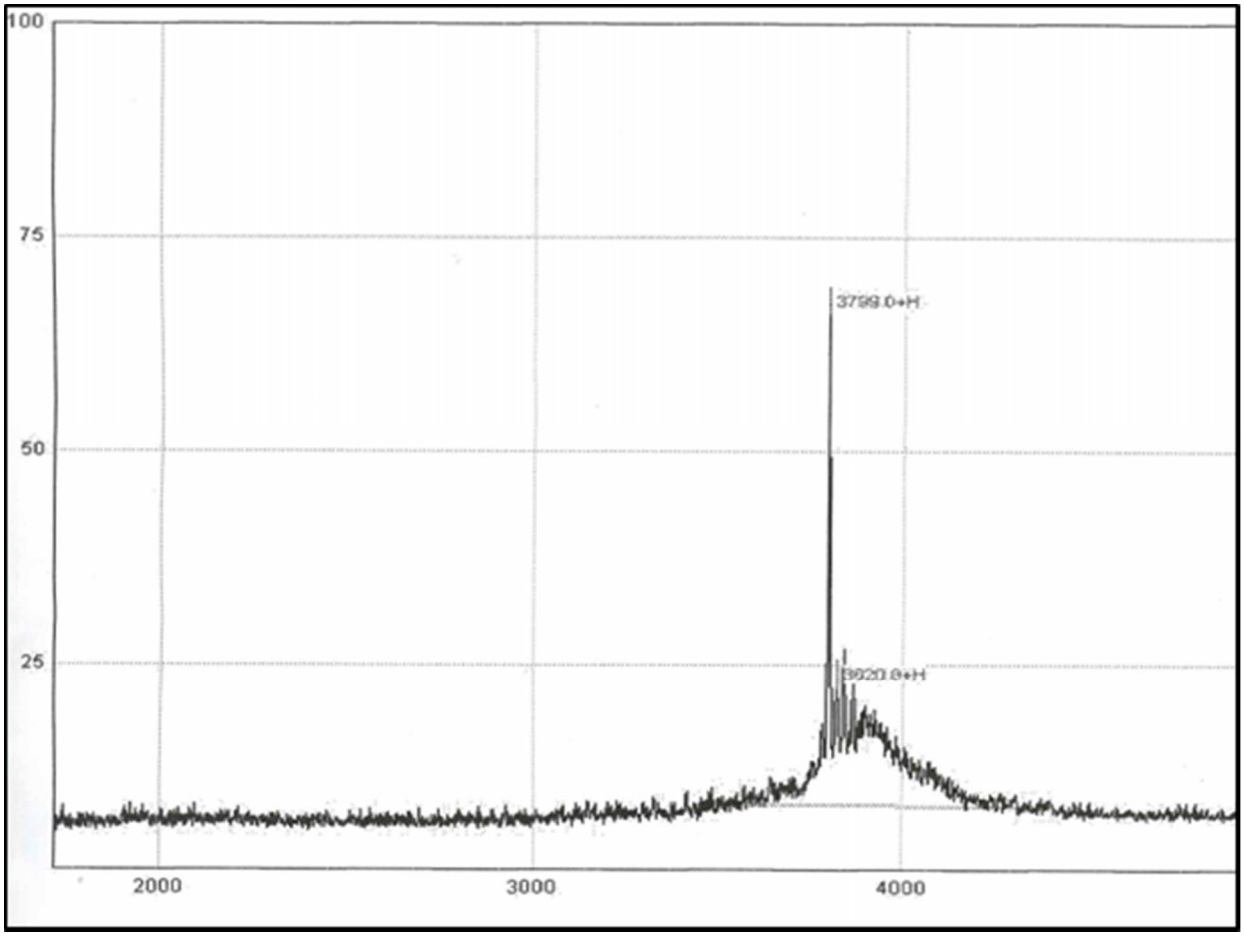

Supplementary Figure 1d. MALDI –TOF characterization of purified VSOR, GRRRAAPEDLYK(5FAM)DFLTGRKKRRQRRRPQ.

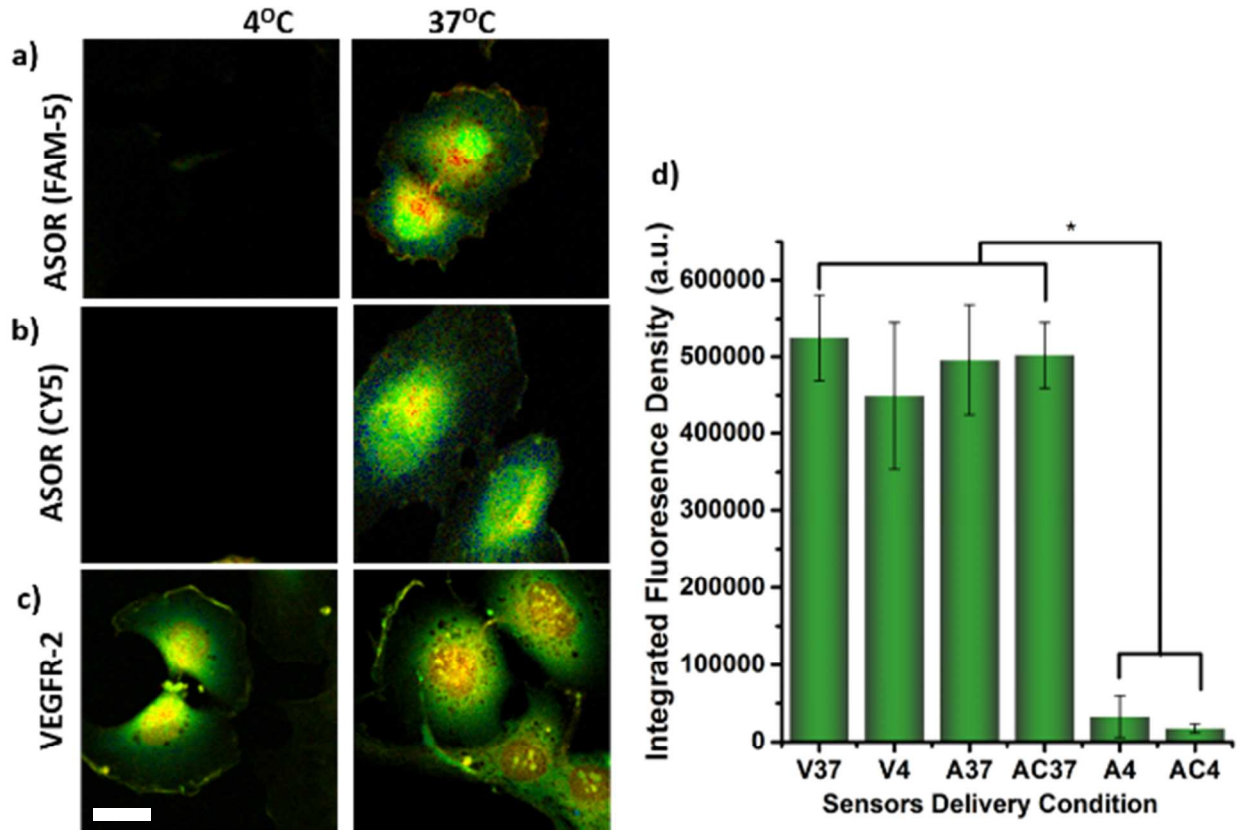

Supplementary Figure 2. Two different cellular uptake mechanisms of ASOR and VSOR in ECFC. Two different types of ASOR sensors, one with a 5-FAM reporter (a) and the other with a CY5 reporter (b), internalized at 37°C suggesting an energy-dependent uptake mechanism of ASOR regardless of the fluorophore reporter (a, b, d). VSOR was rapidly internalized by ECFC at both 4°C (V4) or 37°C (V37) indicating an energy-independent transport of VSOR across the cell membrane (c). (d) Quantified average fluorescence intensity of the internalized sensors in ECFC cells revealed; (1) Cellular ASOR fluorescence intensity at an uptake temperature of 37°C (A37 and AC37) is found to be significantly higher (100 folds) compared to the cellular ASOR fluorescence intensity at 4°C uptake temperature (A4 and AC4). (2) There is no significant difference between VSOR fluorescence intensity at 37°C uptake (V37) compared to VSOR intensity at 4°C uptake (V4), (3) There is a significant difference ($P=1x10^{-10}$) in VSOR intensity at an uptake temperature of 37°C compared to 4°C. Scale bar = 20 um.

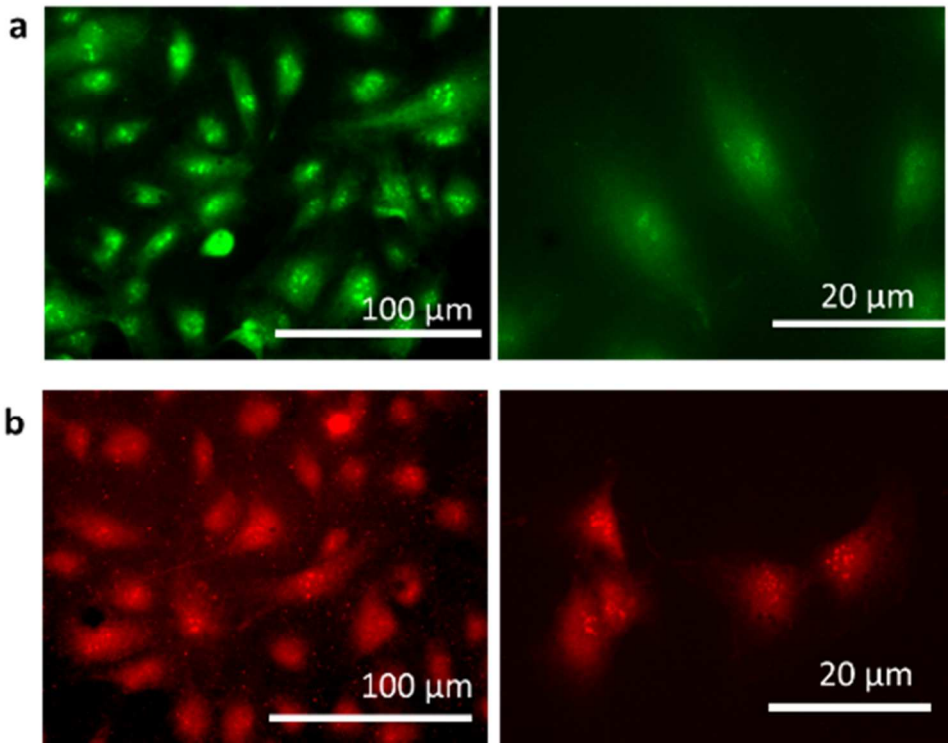

Supplementary Figure 3. Subcellular localization of AKT and VEFGR-2 in ECFC visualized by immunofluorescence. Both VEGFR-2 (a) and AKT (b) are localized in the nucleus, cell membrane and cytoplasm, consistent with the subcellular localization of ASOR and VSOR. The observation was consistent throughout all samples (n=100 cells).

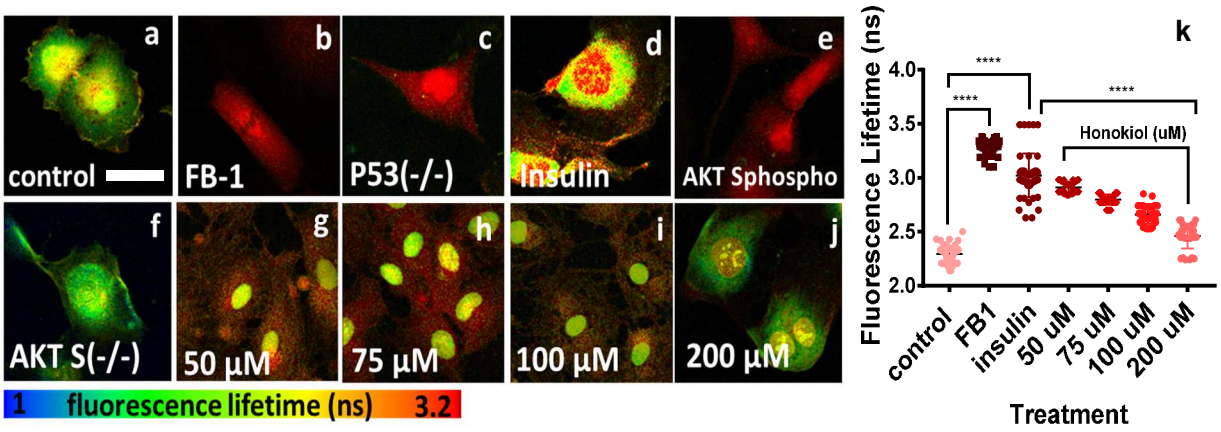

Supplementary Figure 4. Fluorescence lifetime of ASOR depends on AKT phosphorylation. Positive controls for ASOR (b-e) show higher average florescence lifetime compared to control (a, 2.3 ns). (b) 5 µM treatment with FB-1 (3.3 ns), (c) MCF12 p53 (-/-) with constitutively active AKT (3.4 ns), (d) 100 ng/mL Insulin (3.1 ns), (e) phosphorylated Serine ASOR (3.5 ns) (f) Negative controls for ASOR, mutated non-phosphorylatable ASOR (2.4 ns) show decreasing average fluorescence lifetime compared to cells stimulated with FB1 (3.3 ns). (f) treatment with Honokiol, an AKT inhibitor decreases the fluorescence lifetime of ASOR in a dose-dependent manner (g) 50 µM (2.85 ns), (h) 75 µM (2.75 ns) (i) 100 µM (2.5 ns) (j) 200 µM (2.4 ns). (k) Summary of ASOR fluorescence lifetime under different treatments (n=100). (**** P<0.0001). Scale bar = 20 um.

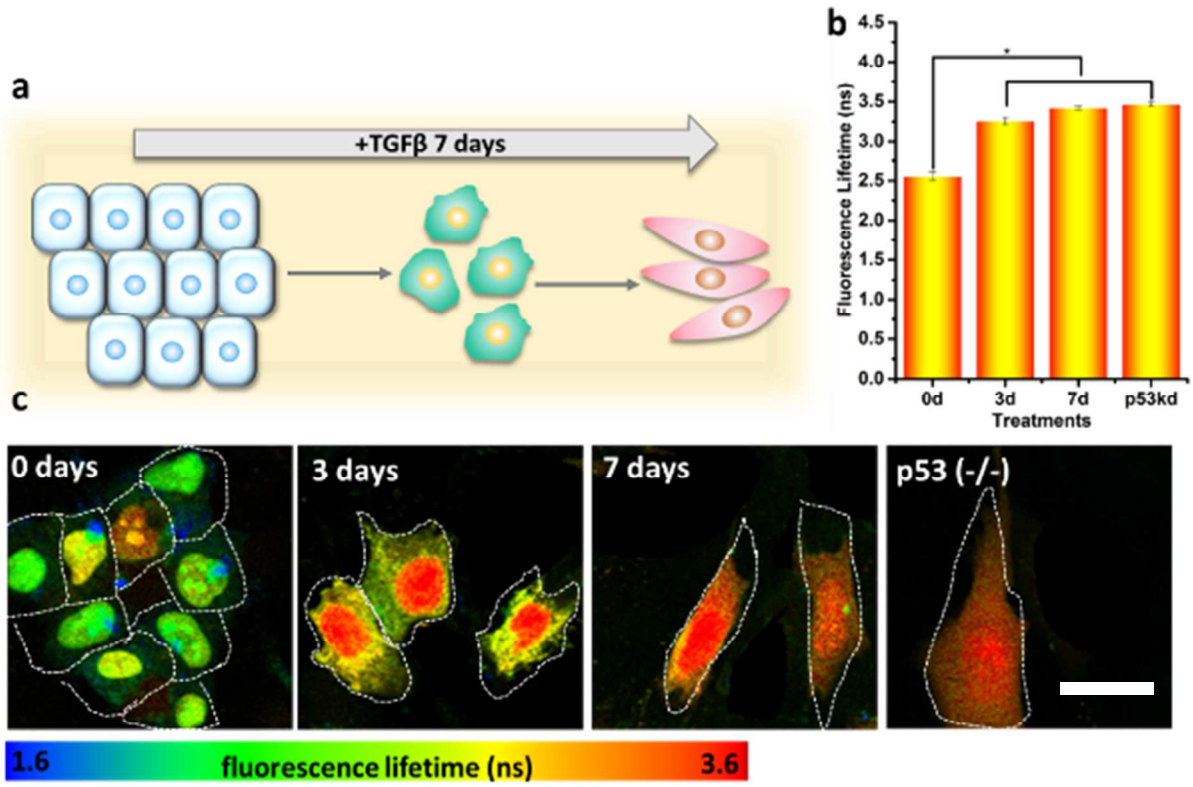

Supplementary Figure 5. Stimulating cells with TGF-β increased the fluorescence lifetime of ASOR in MCF12A. (a) Schematic depicting cell morphogenesis during the 7-day TGF-β treatment. TGF-β activates AKT and can drive cell morphogenesis towards mesenchymal phenotype changes. (b) Quantitative analysis reveals an increased average fluorescence lifetime of ASOR at later time points, (3 days = 3.2 ns, 7 days = 3.4 ns) compared to baseline conditions, cells at initial treatment with epithelial phenotype (0 days, no TGF-β, 2.5 ns). (c) Engineered mutant cells of MCF12 A p53(-/-) with constitutively active AKT shows increase in ASOR fluorescence lifetime (3.48 ns). Summary of ASOR fluorescence lifetime at different time points (n=100). Scale bar = 50 um.

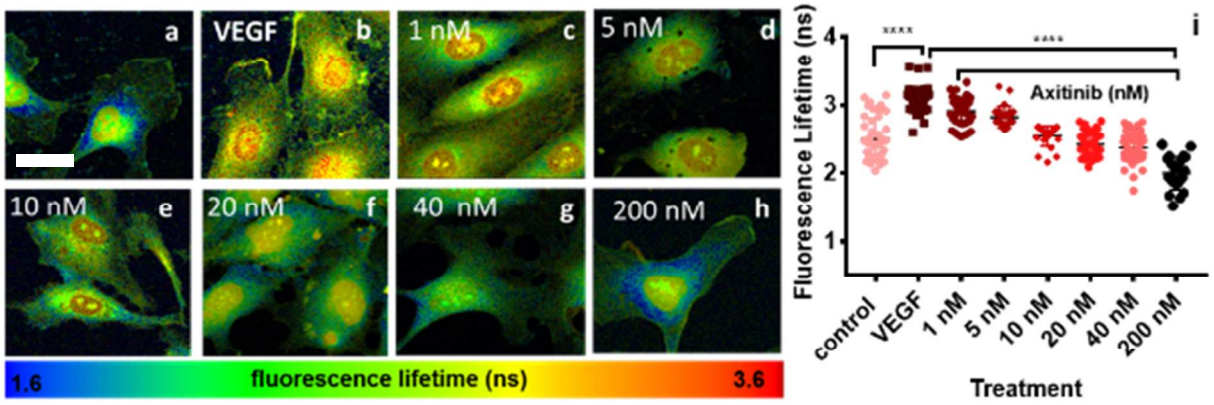

Supplementary Figure 6. Fluorescence lifetime shifts of VSOR depends on VEGFR-2 phosphorylation. Compared to (a) control (2.5 ns), (b) 20 ng/mL VEGF treatment increased the average VSOR fluorescence lifetime (3.3 ns). Treatment with a VEGFR-2 inhibitor, Axitinib, served as the VSOR negative control and showed a decrease in average fluorescence lifetime compared to VEGF-stimulated cells in a dose dependent manner: (c) 1 nM (2.85 ns), (d) 5 nM (2.75 ns), (e) 10 nM (2.5 ns), (f) 20 nM (2.4 ns), (g) 40 nM (2.3 ns), and (h) 100 nM (1.89 ns). (i) Summary of all the average VSOR fluorescence lifetimes (**** P<0.0001). Scale bar = 20 um.

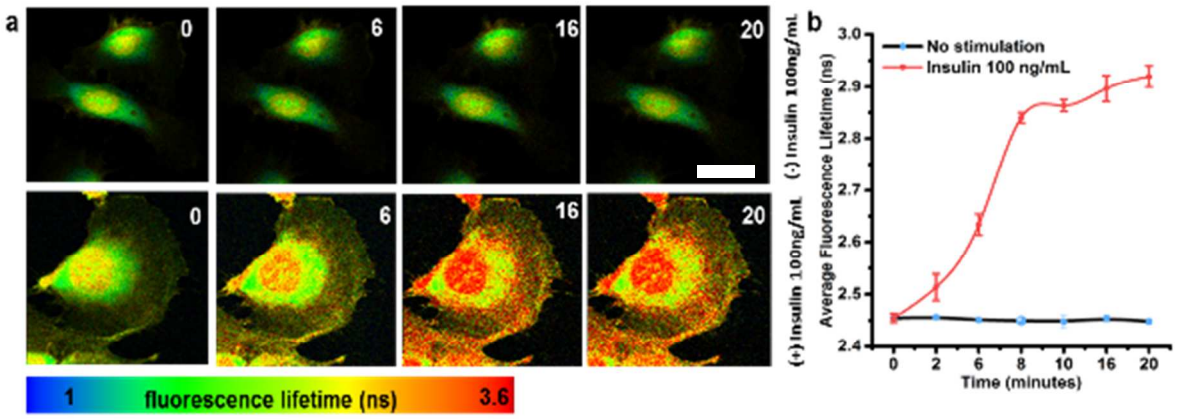

Supplementary Figure 7. Fluorescence lifetime of ASOR responds to insulin stimulation in ECFC. (a) 20-minute time course images show higher average florescence lifetime in ECFC treated with insulin (bottom) compared to control (top). (b) By quantitative analysis we show that the control does not yield any noticeable change in average lifetime over a 20-minute time course (black line). This observation is representative of three technical and three independent biological replicates. Scale bar = 20 um.

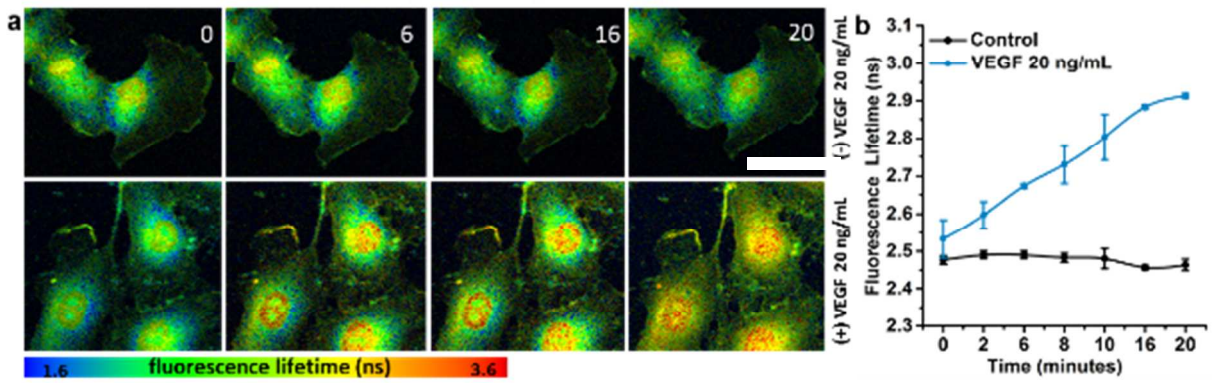

Supplementary Figure 8. Time-course fluorescence lifetime measurements of VSOR activity in ECFC stimulated by VEGF. (a) 20-minute time-course images show higher average florescence lifetime in ECFC treated with VEGF (bottom) compared to control (top) (b) Quantitative analysis confirmed that ECFC treated with VEGF (blue line) not only has a higher average fluorescence compared with the control (non-stimulated cells), but also undergoes detectable changes from the initial average fluorescence lifetime (2.455 ns to 2.94 ns). On the other hand, the control (black line) does not show any noticeable change in average lifetime over the 20-minute time course. This observation is representative of three technical and three independent biological replicates. Scale bar = 50 um

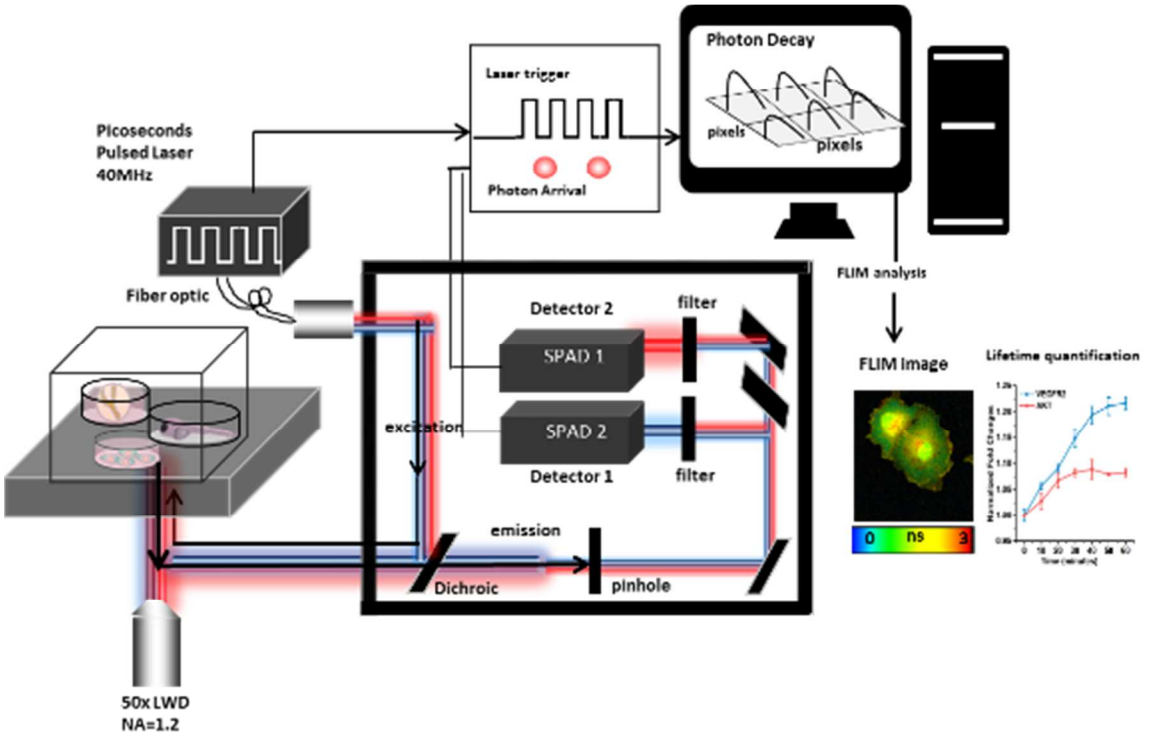

Supplementary Figure 9. Schematic of Time Correlated Single Photon Counting Fluorescence Lifetime Imaging (TCSPC-FLIM) system (PicoQuant, Germany). Excitation was realized by pulsed picosecond diode laser (460 nm and 637 nm; 40 MHz). The laser was coupled to the MicroTime 200 Unit. Images were acquired by raster scanning with XY-Piezo nanopositioning stage (Physik Instrumente, Germany), which allows X-, Y-, and Z-movement precision with 80 µm range and X, Y, Z resolution less than 10 nm. Laser beam was reflected toward the objective using a dichroic mirror (1P-dichroic, Chroma) and then focused into the sample with a long working distance objective (50x, 1.2 NA, Olympus). Emitted fluorescence was collected by the same objective and the emission wavelength was transmitted by a dichroic mirror (1-P-dichroic, Chroma). The emitted light was guided through a 50 µm pinhole and directed into two single photon avalanche diode detectors (SPAD, SPCM-AQR, PerkinElmer Inc.). A 520±60 nm emission filter was placed in front of SPAD 1 to collect signals from 5-FAM while a 685±50 nm filter was placed in front of SPAD 2 to collect emission from the Cy5 fluorophore. The emitted photons were then processed by Time Harp 260 PC-board (PicoQuant, Germany) using time correlated single photon counting method. The photon data was then stored in the Time Tagged Time Resolved (TTTR) mode. The pixel by pixel data was further fitted using SymphoTime software.

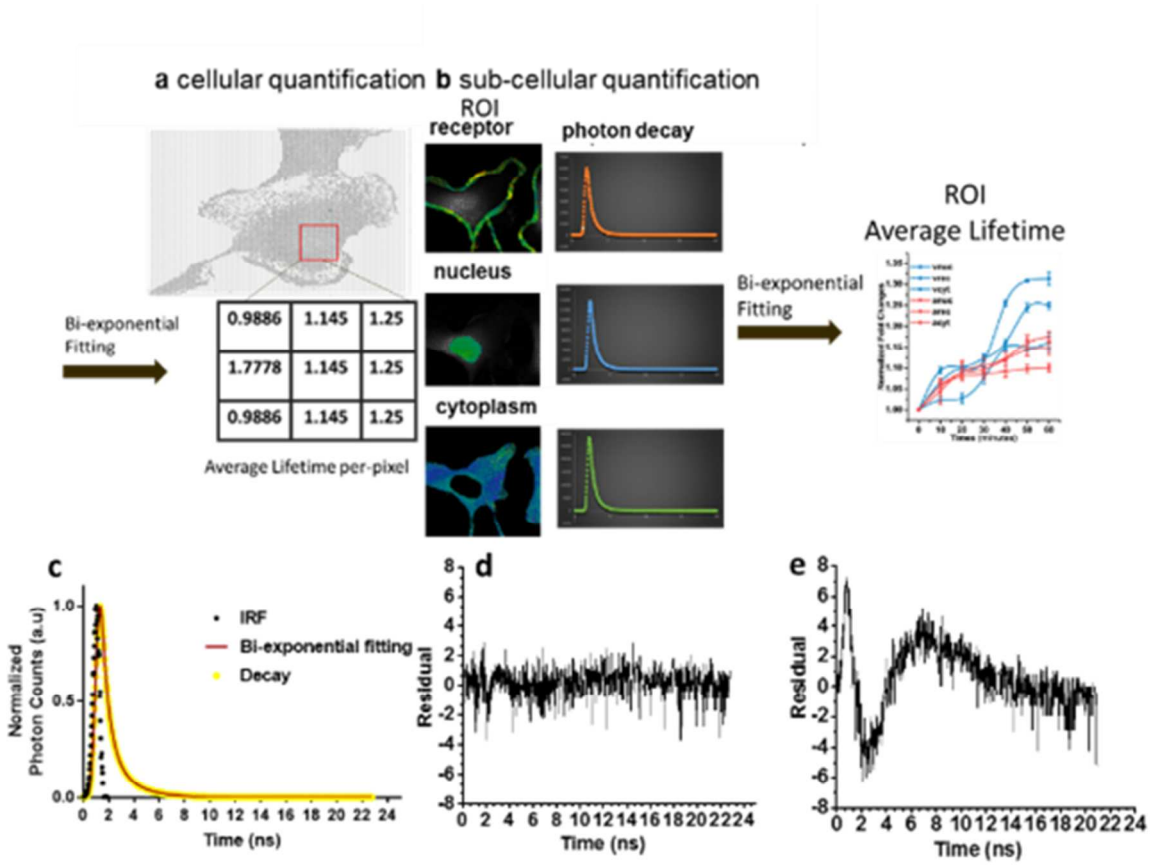

Supplementary Figure 10. FLIM images collected with TCSPC was fitted pixel by pixel to map lifetime information within a cell. (a) Average lifetime per cell was determined by averaging the lifetime of 22,500 pixels. (b) For subcellular quantification, fluorescence decay curves at each designated region of interest was fitted to obtain average lifetime. (c) Example of TCSPC fitting with a bi-exponential model employing Levenberg-Marquadt algorithm. Fitting was performed such that the Chi value is small (<1.3) and no residual deviation from the baseline was observed (d). (e) Example of residual plot from fitting of the same decay curve in (c) using mono-exponential decay model, with a Chi value > 1.3 and distorted residual.

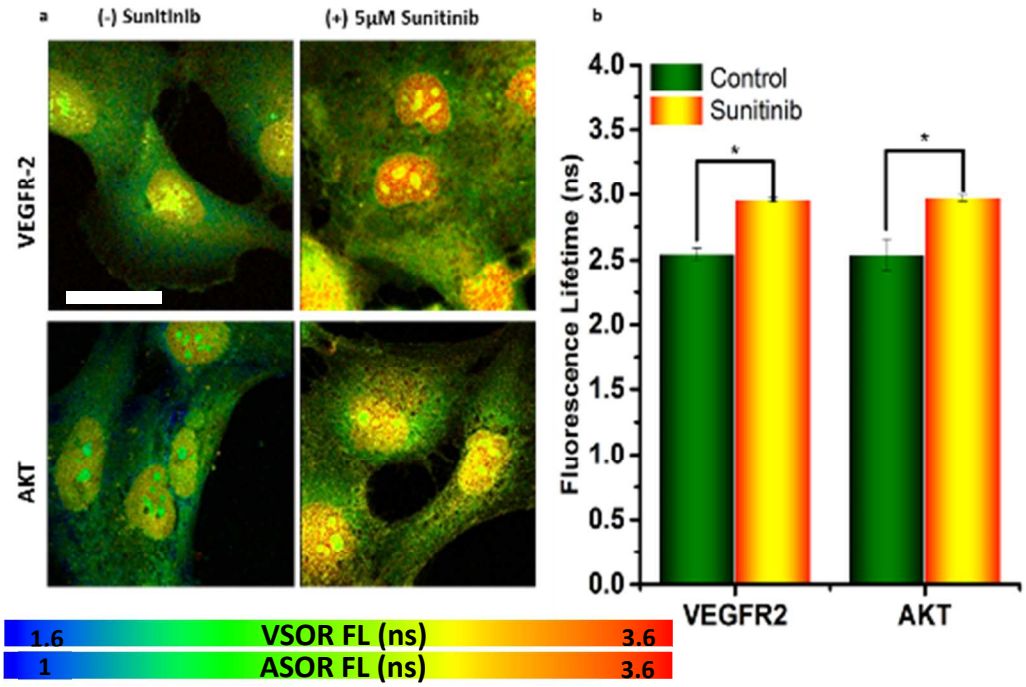

Supplementary Figure 11. VEGFR Inhibition (via 24-hour 5 μM Sunitinib treatment) leads to AKT activation in Sunitinib-resistant 786-R cells. (a) After treatment, fluorescence lifetime of both VSOR and ASOR increased in 786-R cells, (b) After treatment, a statistically significant increase ($P=2x10^{-5}$) in VSOR fluorescence lifetime was observed (2.88 ns vs 2.48 ns as in control). A similar change was observed in ASOR fluorescence lifetime ($P= 2x10^{-6}$) upon treatment (2.9 ns vs. 2.5 ns as in control). Scale bar = 50 μ.

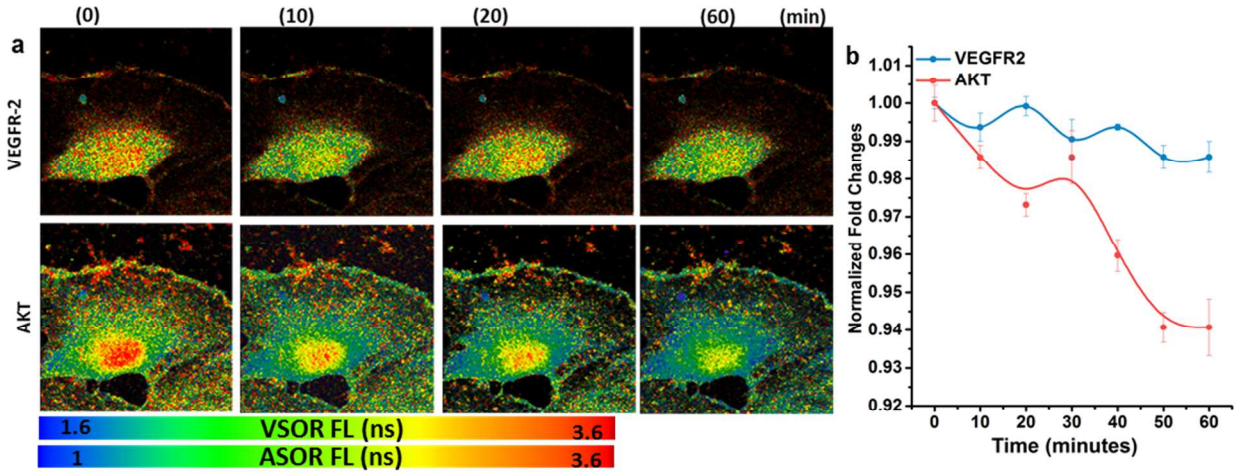

Supplementary Figure 12. Real-time monitoring of ASOR and VSOR after 1-hour of AKT inhibition (treatment with 100 µm Honokiol). (a) Time-course FLIM images of VSOR (top) and ASOR (bottom) show an overall trend of decreasing fluorescence lifetime for both sensors, although a noticeable increase in VSOR fluorescence lifetime was noted after 20 minutes. (b) Quantitative analysis shows a larger decrease in the fluorescence lifetime of ASOR after Honokiol treatment, which is followed by a relatively smaller decrease in the fluorescence lifetime of VSOR. VSOR shows oscillating response starting from 20 minutes with a general decreasing trend. Data is representative of three independent biological and three technical replicates. Scale bar = 50 um.

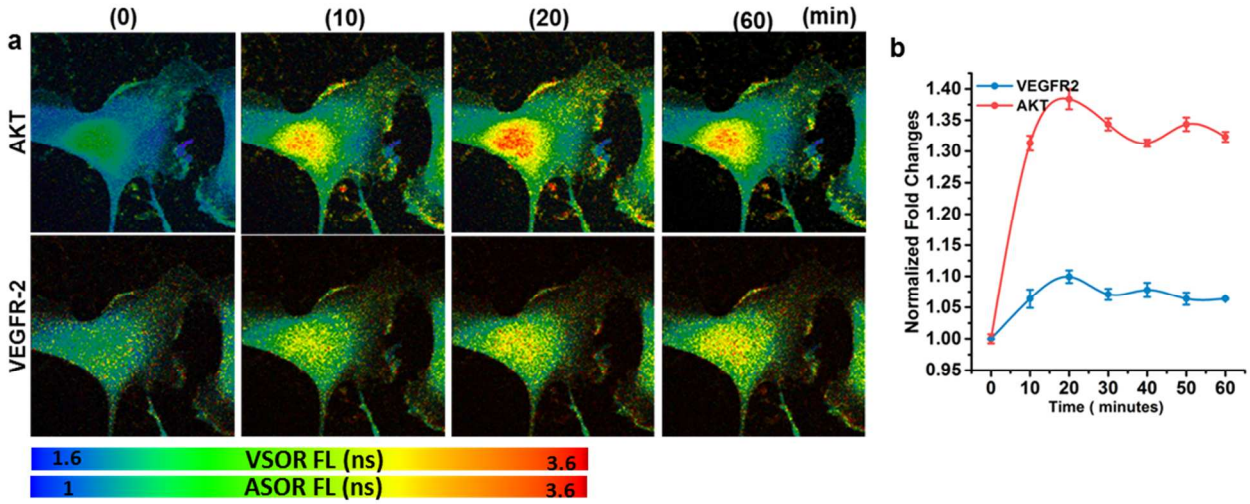

Supplementary Figure 13. Real-time monitoring of ASOR and VSOR after 1-hour of AKT stimulation with 100 ng/mL. (a) Fluorescence lifetime of VSOR (top) and ASOR (bottom) shows an initial increase during the first 20 minutes, followed by an oscillatory behavior for the remaining time period. (b) Results drawn from the qualitative images were validated by quantifying the relative change in fluorescence lifetime in both the sensors. In the first 20 minutes, fluorescence lifetime of both sensors increased, however the increase in ASOR (red line) was greater than VSOR (blue line). After 20 minutes, both sensors exhibited a decreasing oscillatory response. Data is representative of three independent biological and three technical replicates. Scale bar = 50 um.

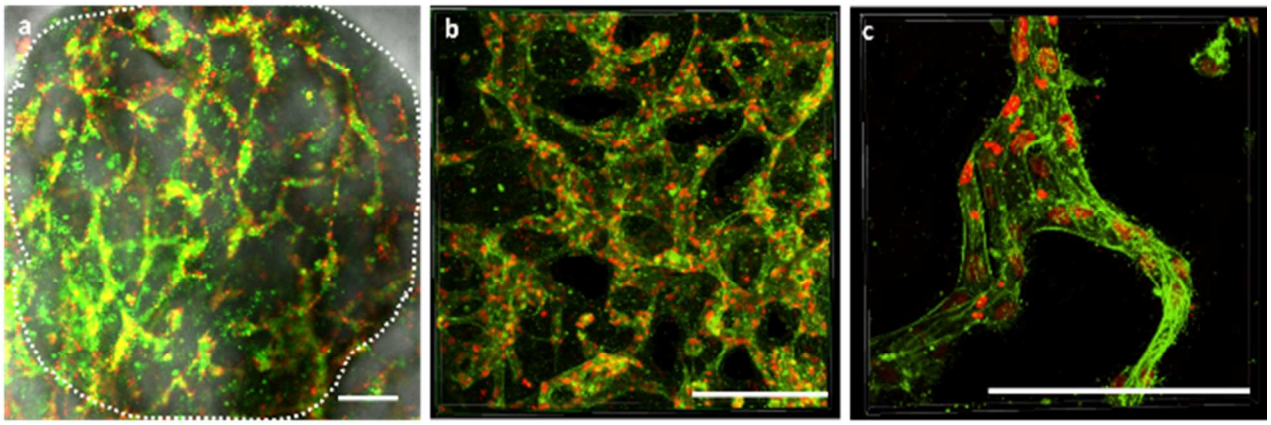

Supplementary Figure 14. 3D vascular structure formed by ECFC. (a) Micro vessel network formed in 3D vasculogenesis model after 3 days of culture. Phalloidin (green) and Hoechst (red) stained for visualization of F-actin and nucleus, respectively with (a) 10x objective, (b) 20x and (c) 60x objective. Scale bar = 100 μm

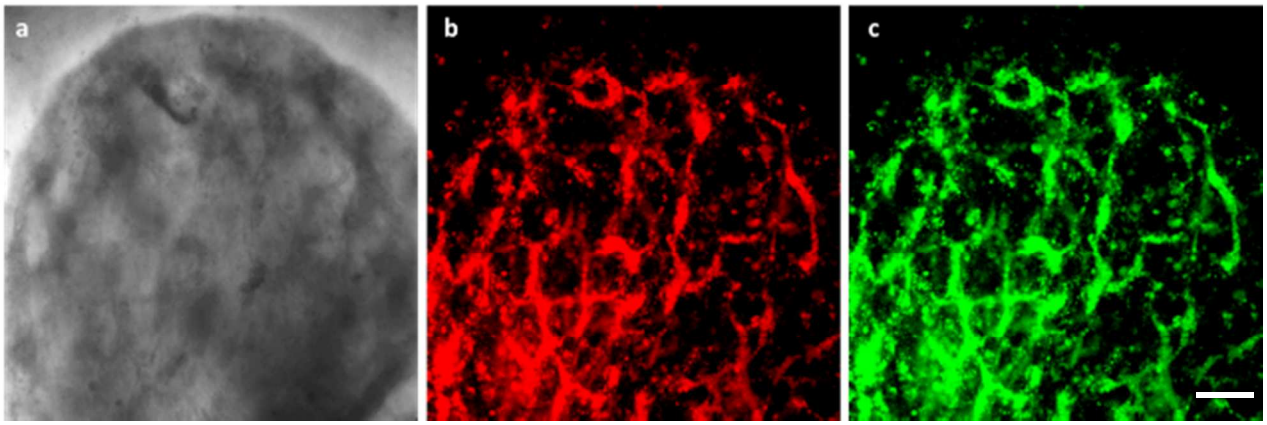

Supplementary Figure 15. ECFC cells in formed vessels successfully internalize ASOR and VSOR after 30 minutes of incubation with 15 μM of each sensor. 10x magnification images of 3D vasculogenesis model from (a) the bright field mode, (b) the ASOR fluorescence channel and (c) the VSOR fluorescence channel. Scale bar = 100 um.

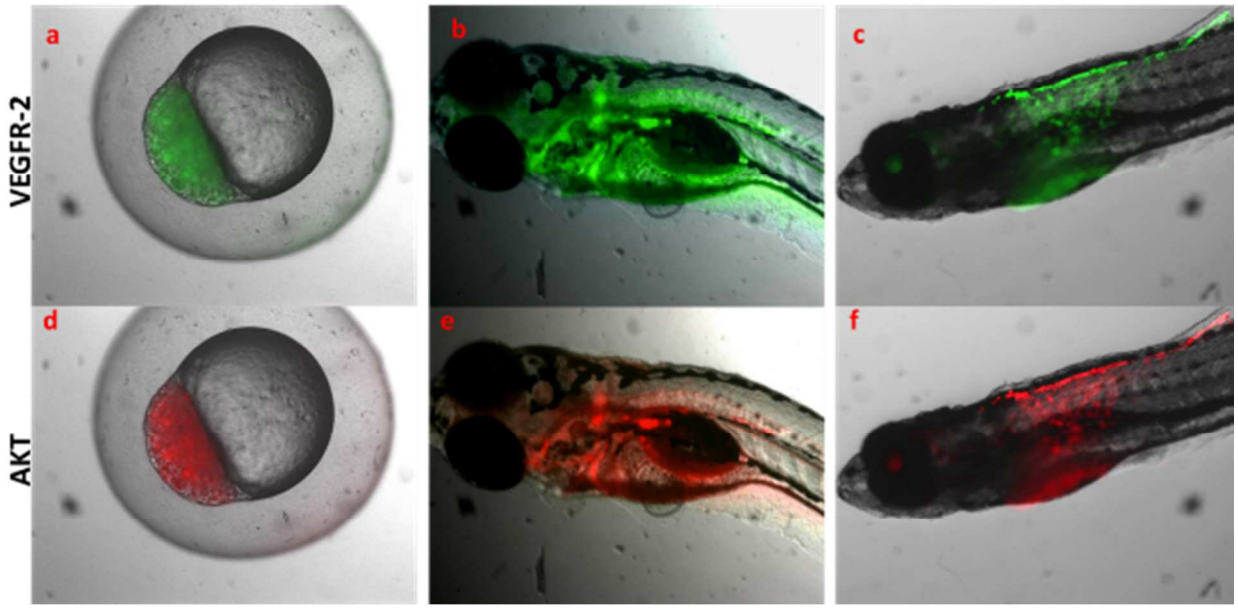

Supplementary Figure 16. Distribution of ASOR (bottom-red) and VSOR (top-green) 10 minutes after the sensor was microinjected into zebrafish at different stages of development. (a, d) 3-hour post fertilization (3hpf) embryo; (b, e) five days post fertilization (5dpf); and (c, f) seven days post fertilization (7dpf).

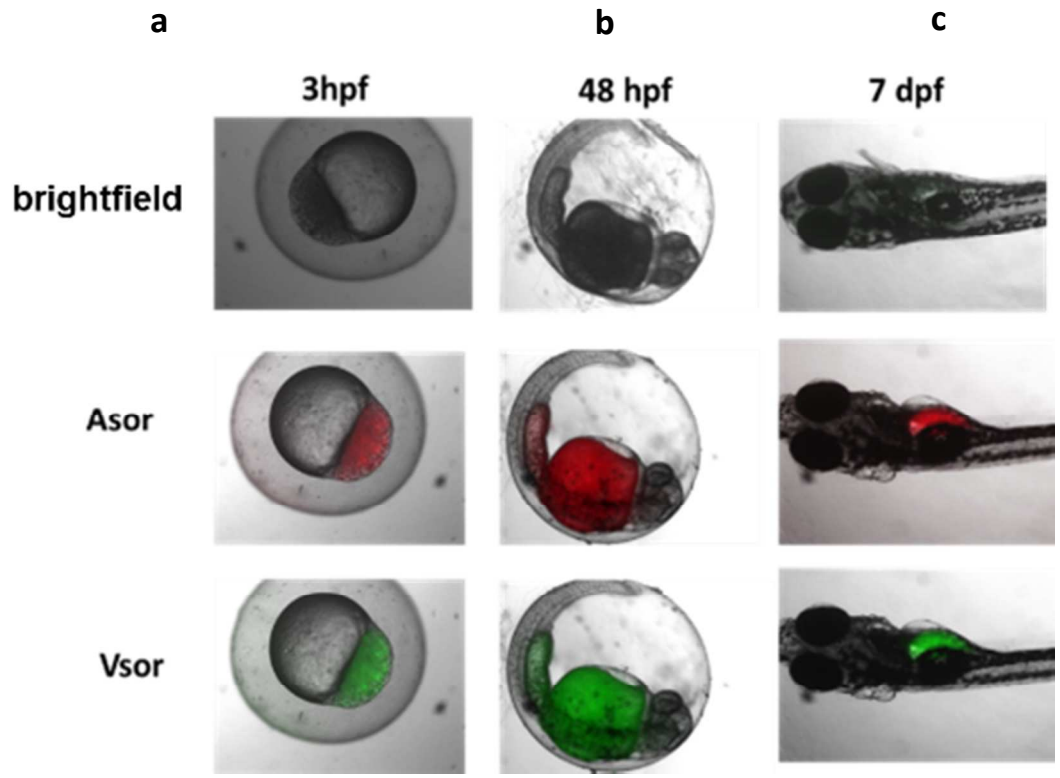

Supplementary Figure 17. Biocompatible evaluation in developing zebrafish after biosensor uptake. Biosensor was microinjected into (a) 3hpf embryo and returned into culture (Egg water, 27°C). Embryo was then imaged at (b) 48 hpf and (c) 7 dpf. All returned embryos (n=5) successfully developed into larvae and no changes in phenotype were observed compared to control.